QUENCH - SAFEST: Scientific Report NUSAFE 3582

Initial assessment of MELCOR Nitriding Model using Air Ingress Experiments QUENCH-16 and QUENCH-18

J. Birchley*, J. Stuckert**, M. Steinbrueck**

*Formerly Paul Scherrer Institut (PSI), Switzerland

**Karlsruhe Institut für Technologie (KIT), Institut für Angewandte Materialien (IAM-AWP)

Programm Nukleare Sicherheitsforschung

Karlsruher Institut für Technologie

Karlsruher Institut für Technologie

in der Helmholtz-Gemeinschaft

Wissenschaftliche Berichte

NUSAFE 3582

Initial assessment of MELCOR Nitriding Model using Air Ingress Experiments QUENCH-16 and QUENCH-18

J. Birchley*, J. Stuckert**, M. Steinbrueck**

*Formerly Paul Scherrer Institut (PSI), Switzerland

**Karlsruhe Institut für Technologie (KIT), Institut für Angewandte Materialien (IAM-AWP)

Programm Nukleare Sicherheitsforschung

Karlsruher Institut für Technologie

2024

DOI: 10.5445/IR/1000170208

Impressum

Karlsruher Institut für Technologie (KIT)
Institut für Angewandte Materialien
Angewandte Werkstoffphysik IAM-AWP
Nukleare Sicherheitsforschung (NSF)
Hermann-von-Helmholtz-Platz 1
76344 Eggenstein-Leopoldshafen
www.iam.kit.edu/awp

Abstract

The impacts of air ingress on nuclear safety have been a matter of concern for some forty years, and particularly so following such an incident at the Paks nuclear power station. As part of the effort to address these issues, an initial assessment of the recently developed PSI nitriding model was performed against the KIT air ingress experiments QUENCH-16 and -18. The study follows on from an experimental investigation on nitriding/reoxidation and the development of a model based on the results and its implementation into a version of MELCOR/1.8.6. The work was motivated by the extensive nitriding observed in previous integral experiments that were originally performed to address oxidation in air.

QUENCH-16 included a period of pre-oxidation in steam followed by an air (without steam) environment to address the continuing escalation up to and past the onset of oxidant starvation, after which nitriding is expected. QUENCH-18 was an approximate counterpart experiment in which the environment following pre-oxidation comprised a mixture of steam and air.

The capability to model the effect of a mixture of steam and air, addressed in QUENCH-18, is investigated qualitatively by repeating the QUENCH-16 simulation with the additional of steam flow corresponding to the QUENCH-18 conditions. An exact quantitative comparison between the QUENCH-16 and -18 results is not possible because of differences in bundle configuration.

Comparison between the QUENCH data and MELCOR simulations with and without the nitriding model show how the code captures the main trends and that the model captures the uptake of nitrogen and heat generation after all the oxygen is consumed, with formation of zirconium nitride (ZrN). No significant uptake of nitrogen was observed before oxygen starvation, in either the experiments or simulations. However, some nitrogen uptake was observed before steam starvation in QUENCH-18.

Some calculational difficulties emerged during the late stages of the simulations, including reflood, which are thought to be due to numerical issues. There is also an unintended difference in the calculated oxidation rate, due to an incorrect numerical treatment of the kinetics. Recommendations are proposed to address these shortcomings.

Contents

1. Introduction

One of the potential impacts of air ingress to overheated fuel during a reactor or spent fuel accident is the formation of zirconium nitride (ZrN). The reaction is not only a source of heat, but the ZrN itself reacts readily and exothermically with oxygen, steam or even liquid water, with the release of nitrogen. The formation of nitride, even in trace amounts, causes the oxide layer to lose its effectiveness as a protective layer to limit further oxidation.

Concerns over the risks of air ingress was first raised by Powers et al. [1] following the realisation that the TMI-2 reactor vessel had been worryingly close to lower head failure [2]. If the vessel had failed, there would have been a pathway for air to ingress into the already severely damaged core. Air oxidation kinetics became the subject of debate and experimental studies [3]. The main concerns at the time were the effect of accelerated kinetics on the ongoing accident escalation, and the risk that exposure of the fuel itself to oxygen would render certain of the radiotoxic actinides and fission products in a more volatile state.

Further attention was focussed on air ingress sequence following the Paks cleaning tank incident in 2003 [4]. Several experimental programs were launched to investigate the impacts and to characterise the chemical-dynamic processes in order to enable analysis and risks assessments of the associated threats.,

Separate-effects test (SET) programs to furnish basic data were launched at IRSN, France [5] and KIT, Germany [6, 7]. The integral test programs include QUENCH (KIT, Karlsruhe, Germany) [8], PARAMETER SF4 (Luch, Russia) [9], CODEX AIT (AEKI, Hungary) [10], and the SFP-1 and -2 (Sandia National Labs, USA) [11]. To begin with the main issue regarding core damage escalation was considered to be the accelerated oxidation kinetics due to the effect of nitrogen on the integrity of the oxide layer. However, several of the later integral tests demonstrated very significant nitriding with major impacts on subsequent coolability.

In particular, the QUENCH-16 [12] and QUENCH-18 [13] experiments, with air oxidation under starvation of oxidant, yielded data which showed extensive formation of zirconium nitride followed by strongly enhanced hydrogen production during the quenching process with water, and also release of nitrogen. SETs with air oxidation under oxygen starvation conditions also showed presence of zirconium nitride in the post-test examination [14, 15]. The Sandia Fuel experiments showed strong nitrogen uptake during the oxygen starvation stage of the experiments and nitrogen release during re-oxidation of the zirconium nitride later on. This behaviour was a challenge for the severe accident codes, for example the benchmark exercise on the Sandia experiments [16], since models for the nitrogen/nitride reactions were limited or, in some codes, unavailable, e.g., MELCOR and SCDAP.

With the recognised need for a nitriding/reoxidation model for use in MELOR, PSI (Switzerland) and KIT (Germany) launched a two-part project to address the need. The first part was to obtain empirical data on the reactions between zirconium-based alloys and air in the frame of a PhD project [17], [18]. The second part was to apply the data to support development of a computer model to describe the reaction processes and their kinetics [19] and to implement it into a PSI version of MELCOR1.8.6 [20]. This code version already included models for breakaway oxidation in steam and accelerated kinetics in the presence of nitrogen [21], which had previously been extensively assessed against PARAMETER-SF4 [9] and QUENCH air ingress experiments [22, 23], provided a framework within which to implement the nitriding model. The new nitriding version was recently applied to a hypothetical spent fuel pond accident [24]. Following on from the model development, and in parallel with the application, a first independent assessment was performed making use of integral transient data, namely experiments QUENCH-16 and -18. The resulting simulations are the subject of the present paper.

MELCOR simulations of the QUENCH air ingress experiments was a natural choice for assessing the nitriding model, since the code and input model had been used previously for several QUENCH experiments and were well validated for a range of conditions. In particular it was one of the codes used in the QUENCH-10/-16 benchmark exercise [23], performed in the frame of the EU SARNET programme. The two experiments used the same test section specifications and the same MELCOR model was used in the benchmark, differing only in the boundary conditions which were slightly idealised for QUENCH-16 to reflect the nominal test protocol. A number of unplanned and unquantified variations and also the breach of the shroud at the time of reflood were ignored.

The benchmark model was therefore a natural starting point for the present assessment study. Conceptually, QUENCH-18 was a counterpart of -16, differing only in that a flow of steam was included during the air ingress phase. However, pragmatic considerations meant a slightly different specification of the section configuration. Following extensive planning analyses [25], it was possible to specify the boundary conditions expected to result in a very similar pre-oxidation transient. The added steam makes for a more complicated set of reactions, and a sterner test of the model capability. It can be reasonably argued that the steam-air mixture is more representative of an actual reactor or spent pool scenario. There also a scarcity of data for such conditions, as air ingress experiments are typically performed in the absence of steam, including those used to develop the model. QUENCH-18 is the only experiment known to the authors in which an air-steam mixture was used. Consequently, some aspects of the model are not supported by empirical data.

It is stressed that the primary goal of the study was not to reproduce the experimental data, rather to assess applicability of the model to sequences of this kind, and to check how well the model works as intended. An important element of this was to examine the model's effectiveness in simulating the behaviour in a steam+air environment compared with an air environment, under otherwise similar conditions.

The present assessment study was presented at the 27th International QUENCH Workshop [26], and this paper is essentially a more complete and formalised account. The following section presents and compares the experimental results used to provide the reference data. Section 3 identifies the analytical tools, summarises the reaction scheme, identifies the separate cases with their respective modelling choices, and describes how the QUENCH model and boundary conditions are used in the simulations. Section 4 presents the calculated results and compares the simulations with each other and with the experimental data. Section 5 briefly summarises the key observations. Conclusions from the study and recommendations for future work are presented in section 6.

2. Experimental background

The QUENCH facility, operation and the present experiments have been extensively documented elsewhere [8], and are not repeated here. Before discussing the calculations, however, it is helpful to summarise the key features of the two experiments by means of a side-by-side comparison.

Comparison of QUENCH-16 and -18 configuration and operation

The main differences between the bundle configurations and operation are shown in Figure 1 and Table 1. We observe in particular noticeable differences in the physical dimensions and number of heated rods, although there is (importantly) only a small difference in in the flow area and Zr- based surface area.

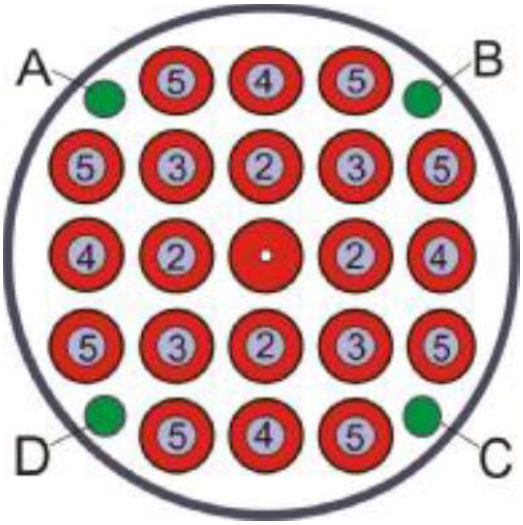

QUENCH-16: 20 heated, 1 unheated rod, 4 solid corner rods

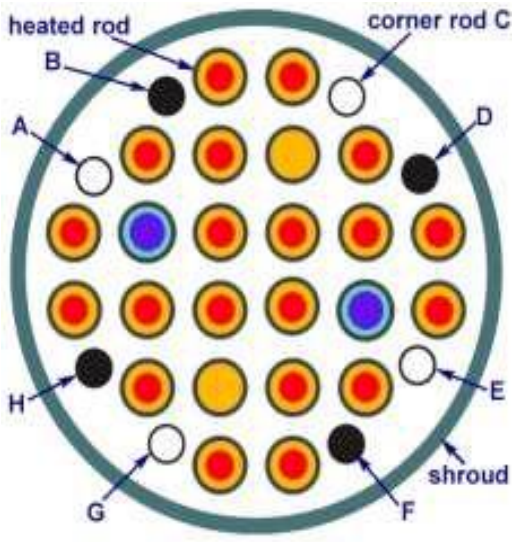

QUENCH-18: 2 heated unpressurised rods, 2 unheated pressurised rods, 2 absorber rods, 8 corner rods (4 solid, 4 hollow)

Figure 1: QUENCH-16 and -18 bundle configurations

Table 1: Comparison of key experimental parameters

Quantity (unit)		QUENCH-16	QUENCH-18	Ratio (18/16)
Shroud inner diameter (mm) Shroud thickness (mm)		82.8 3.05	82.8 3.05	1.0 1.0
Total area inside shroud (cm2)		53.84	53.84	1.0
Flow area (cm2)		33.65	33.55	0.997
Area occupied (cm2)		20.19	20.29	1.005
Wetted perimeter heated (mm)		675	597	0.884
Wetted perimeter unheated (mm)		386.3	565.8	1.465
Wetted perimeter total (mm)		1061.3	1162.8	1.096
Hydraulic diameter (cm)		12.68	11.54	1.099
Number of heater rods OD of rods/heater elements (mm)		20 10.75 / 6	20 9.5 / 5	1.0 0.884 / 0.833
Nominal electrical power during temperature plateau (kW) Gross (incl. external resistance) To heater elements (estimated)		 11.4 8.95 (78%)	 9.4 7.9 (84%)	 0.825 0.883
Preoxidation Steam flow(g/s) Argon flow (g/s)		 3.4 3.0	 3.3 3.0	 0.97 1.0
Air ingress Air flow Steam flow(g/s) Argon flow (g/s)		 0.2 0.0 1.0	 0.2 0.3 1.0	 1.0 - 1.0

Several of the parameters are the same or very similar. The main differences considered most likely to have affected the transient evolution are the heated perimeters, and hence heat transfer area, (ca. 12% lower in -18) and the electrical power to the heaters (ca. 12% lower in -18). We could expect that the two differences would largely offset each other as regards their combined effect on the thermal response. Independent planning calculations [25] using different simulation tools supported the expectation that the QUENCH-16 preoxidation transient would be essentially replicated in QUENCH-18 via a ca. 18% reduction in gross power. The smaller rods in the QUENCH-18 bundle meant that a higher fraction of the gross electrical power was dissipated in the heater elements than in QUENCH-16. The overall efect was that the dimensional ratios of bundle power to heat transfer area was the same for both experiments.

Comparison of QUENCH-16 and -18 experimental signatures

Before discussing the comparison between the simulations and experimental results, we briefly consider the main signatures: temperature, hydrogen generation, and offgas composition. The intermediary cooling, before the switch from steam to air at a lower flow rate (and hence reduced heat transfer),

was because the electrical heating was reduced in order to allow the air ingress transient to develop from temperatures where the oxidation rate is low.

The event sequences, including the transition times between the separate phases - pre-oxidation, air ingress, reflood are given in the experimental reports [24, 25]. Due to the differences between the experiments and simulations, side-by side comparisons are not presented.

Both experiments exhibited high temperatures and significant degradation to both the heater rods and shroud, resulting in numerous thermocouple failures and a scarcity of good temperature data, which meant that comparison for thermal response is somewhat compromised by having to use measurements from different locations. Figure 2 shows the temperatures at 750 mm, on the inner ring heater rod cladding, TFS 5-11, and on the shroud, TSH-11, for QUENCH-16 and -18 respectively. The lower temperatures and slower heat-up/cooldown during preoxidation in QUENCH-18 probably reflect the peripheral location, the larger thermal inertia of the shroud, while the slower subsequent heat-up was due to the higher coolant flow during air ingress. That difference is later reversed by the additional heat by oxidation in steam after oxygen starvation.

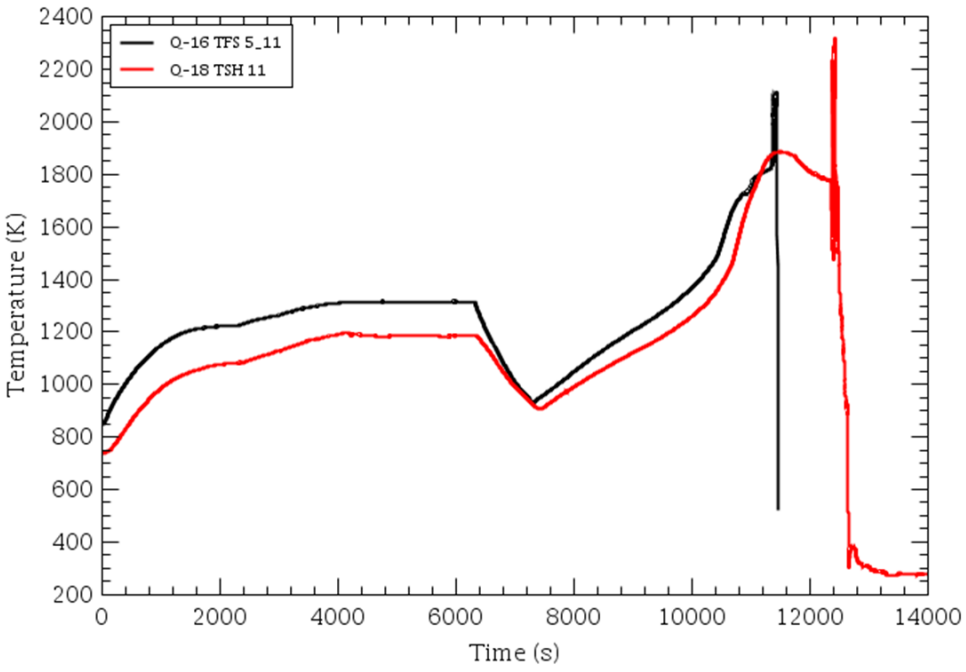

Figure 2: QUENCH-16 and -18 observed experimental temperatures at 750 mm

The hydrogen generation profiles, Figure 3, are similar during pre-oxidation, suggesting broadly similar temperatures, while further hydrogen was generated during the QUENCH-18 air ingress phase following oxygen starvation, at a rate corresponding to the steam flow rate of 0.3 g/s. There was a very small release of hydrogen, about 2 g, at an equivalent time during QUENCH-16, due to a small but unquantified and probably unavoidable flow of steam as previously condensed steam re-evaporated in the dry environment. Both experiments showed major oxidation excursions during reflood.

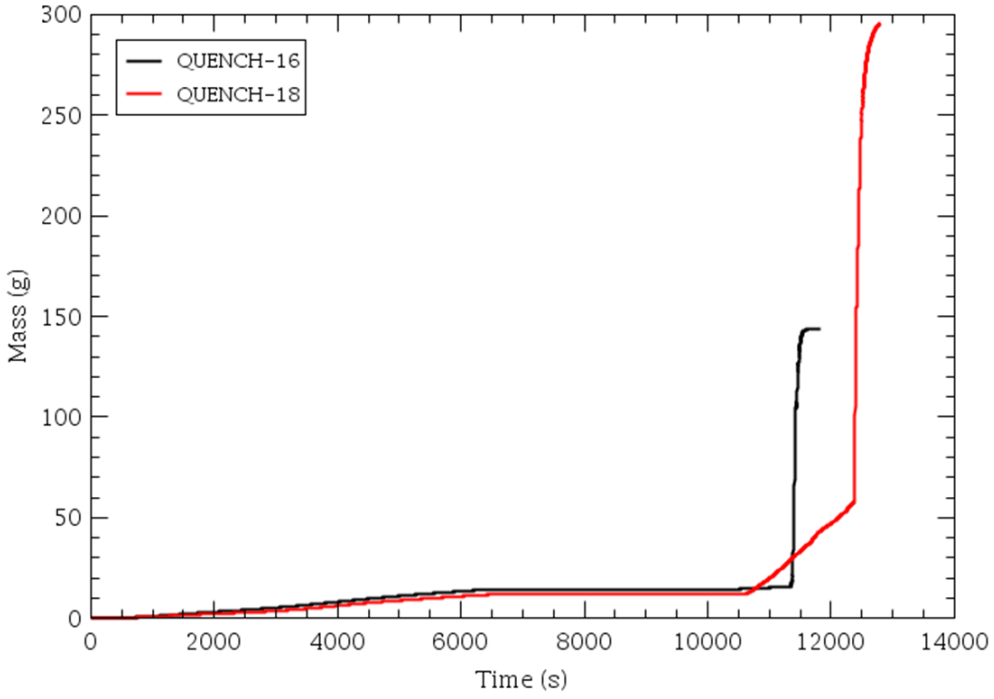

Figure 3: QUENCH-16 and -18 experimental hydrogen generation

The offgas compositions, in terms of molar fraction are compared in Figure 4 for the period after pre-oxidation. The calculated and measured oxygen and nitrogen concentration histories follow parallel trends between the two experiments, but differ in magnitude and timing due to the presence of steam in QUENCH-18. In both experiments nitrogen and steam consumption did not begin until all the oxygen was consumed. Interestingly, nitrogen consumption in QUENCH-18 began while there was still a significant fraction the steam present, but did not become fully consumed in either experiment. A small residual flow of steam in the offgas continued until reflood, possibly for the same reason as in QUENCH-16, and might not have all flowed through the bundle. It is therefore difficult to be certain of the concentration in the bundle and how much was consumed.

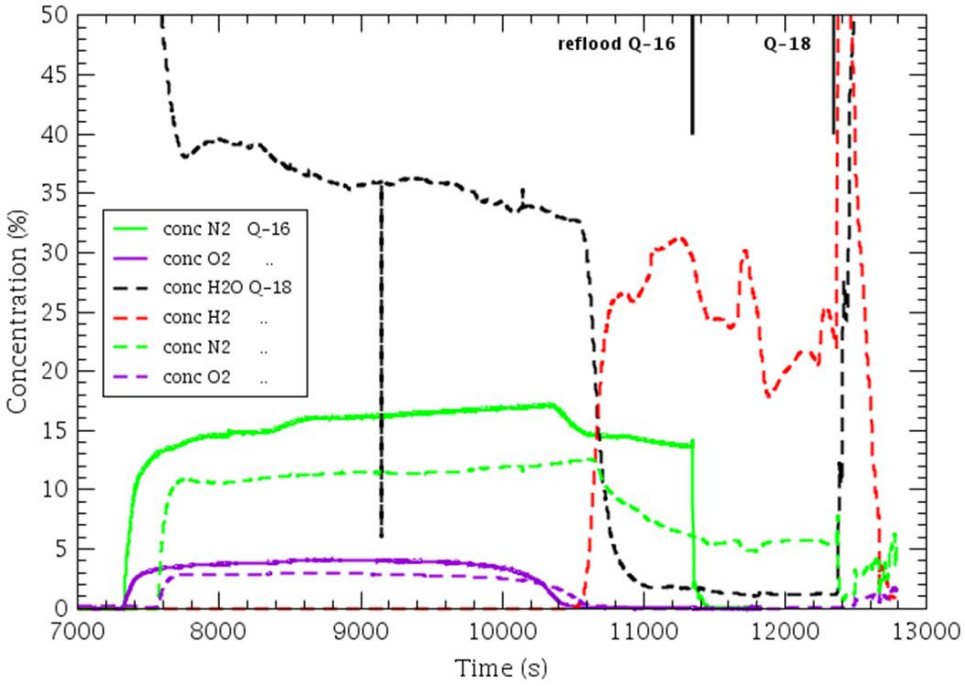

Figure 4: QUENCH-16 and -18 experimental offgas composition

Basis for modelling of the QUENCH experiments and boundary conditions

The input for the QUENCH facility used in the calculations is the same as had been used to analyse several previous experiments, QUENCH-06, -10, etc., using the both the 1.8.5 and 1.8.6 code versions. For QUENCH-16, the model was adapted to reflect the experimental boundary conditions. It was also very slightly idealised to facilitate their use and code-code comparisons in the benchmark exercise carried out by participants in the European ERMSAR programme [23], in which QUENCH-10 and -16 were used as the reference cases. In both experiments there was a period of pre-oxidation in steam followed by a termination of the steam flow and switch to air flows at differing rates (1.0 g/s and 0.2 g/s in -10 and -16, respectively) to investigate the effect of a period of oxygen starvation on the thermal response, nitriding, and coolability. The exact same input, including boundary conditions was used in the present QUENCH-16 calculations to assess the nitriding model.

QUENCH-18 was, conceptually, a counterpart to QUENCH-16 but with continued steam flow during the air ingress phase. In reality there were differences in the test section configuration and cladding materials, though retaining the same essential elements as the earlier experiment. The boundary conditions were modified in such a way as to try to replicate, as far as possible the pre-oxidation phase and hence the starting conditions for the air ingress. In practice this objective was achieved, with only minor differences in the thermal behaviour, the extent of cladding oxidation, and timing of the start of air ingress.

Rather than attempt to model the details the QUENCH-18 experimental set up and boundary conditions exactly, the same input was used as for -16 except that the -18 steam flow was used. This made it possible to examine most easily how well the model captures the influence of a steam-air mixture as opposed to air alone, without needing to take into account the effect of detailed differences between the experimental set ups. It also enabled direct comparison of the calculated air-ingress behaviours with and without activating the nitriding model. It is noted that the primary aim of the calculations is an assessment of the applicability of the model for simulating nitriding/re-oxidation in an air ingress

sequence and capturing the main phenomenology, rather than to specifically compare the calculated results with empirical data. However, the QUENCH-16 model sufficiently replicates the experimental set up that the results can properly be compared with the data as a validation exercise.

To avoid confusion, the QUENCH-18 model used in the present simulations is from now on referred to as QUENCH-18*, an idealised representation of both the experimental test section and conditions.

3. Analytical tools

Summary description of nitriding model

The present simulations were performed with a developmental version of MELCOR-1.8.6/PSI, where the PSI model for breakaway and for accelerated oxidation in the presence of nitrogen, used in previous analyses, has been extended to include also the reactions involving nitrogen with partially oxidised cladding in addition to those with steam and oxygen [19]. The model and its developmental assessment are described in some detail, and only the reaction scheme is summarised here.

The key new features of the model are as follows.

Under oxidising conditions (steam or oxygen), both ZrO_2 and oxygen-stabilised alpha-zirconium, often referred to simply as Zr(O) are formed. The latter is assumed in the model to have the composition, $ZrO_{0.4}$, but in reality the Zr(O) composition varies and $ZrO_{0.4}$ is equivalent to the maximum oxygen content. From now on, we use the chemical symbol “Zr” to refer to elemental zirconium, while the word “zirconium” may refer to either or both.

Under oxidant starved conditions, nitride (ZrN) is formed by the reaction between nitrogen and $ZrO_{0.4}$, with the release of oxygen into the zirconium.

Under subsequent oxidising conditions, the nitride and remaining zirconium are oxidised with release of hydrogen.

The model assumes a strict reaction precedence, i.e., mutually exclusive:

oxidation by oxygen > oxidation by steam > nitriding.

This implies that, locally, oxidation by steam takes place only if oxygen is absent, and that nitriding takes place only if neither oxidant is present. It is noted that the precedence and mutual exclusivity are local, not global. The extent to which this precedence applies in the real situation is a goal for future studies.

The individual reactions are indicated, thus:

$$Zr + O_2 = ZrO_2 \quad (1)$$

$$Zr + 2H_2O = ZrO_2 + 2H_2 \quad (2)$$

Zr(O), which is modelled as having the composition $ZrO_{0.4}$ and from now referred to as such in the discussion of the reaction model, is formed by diffusion, indicated by the conceptual reaction

$$4Zr + ZrO_2 = 5ZrO_{0.4} \quad (3)$$

The diffusion of oxygen from the oxide into the underlying metal has long been studied, and the kinetics are added to standard parabolic correlations [27, 28], although it is not included in MELCOR or in some of the other integral simulation tools.

In the present model, Cathcart-Pawel is used in for the uptaken oxygen mass, separated into two parts, the masses in oxide layer and in the $ZrO_{0.4}$. This somewhat novel feature of the oxidation process compared with the classical parabolic treatment is indicated schematically in Figure 5.

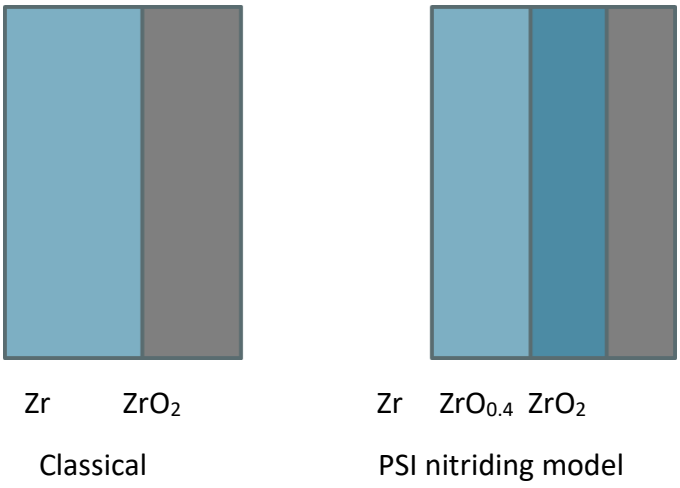

Figure 5: schematic treatment of oxidation in nitriding model.

Recent studies at KIT [29] have shown that $ZrO_{0.4}$ in turn reacts fairly readily with nitrogen to form nitride with the release of intermediary oxygen, according to

$$2ZrO_{0.4} + N_2 = 2ZrN + 0.8[O] \quad (4).$$

Oxygen is not released from the cladding during nitriding. If both Zr and $ZrO_{0.4}$ are present, the model arbitrarily assumes that half of the released oxygen reacts with $ZrO_{0.4}$ to produce oxide and half is taken into the metallic Zr, partially replenishing the $ZrO_{0.4}$. Conceptually, that is

$$0.8[O] = 0.4[O] + 0.4[O]$$

$$(0.4[O] + Zr) + (0.4[O] + 0.25ZrO_{0.4}) = ZrO_{0.4} + 0.25ZrO_2 \quad (5)$$

If the zirconium is entirely $ZrO_{0.4}$, then all the [O] goes to form oxide. Correspondingly, if the zirconium is entirely Zr, then all the [O] goes to form $ZrO_{0.4}$. Clearly, if neither Zr nor $ZrO_{0.4}$ remain, i.e., all the Zr is fully reacted, then the nitriding terminates.

While there is no positive evidence to support above apportioning, it seems likely that the nitriding will consume more $ZrO_{0.4}$ than it produces, with the possibility that little $ZrO_{0.4}$ will remain. The continuation of nitriding then depends on the slow diffusion of oxygen from the oxide to the Zr, which becomes the rate controlling process. A transition was often observed in the experiments between “fast” and “slow” stages of nitriding, interpreted as occurring when the pre-existing $ZrO_{0.4}$ had been consumed. In some cases, nitriding was observed to terminate, interpreted as occurring when all the zirconium has reacted to form oxide or nitride which was supported by post-experiment examinations [19].

If oxidant is available after nitriding, both the zirconium and nitride are oxidised. The zirconium is oxidised in the normal way, while the nitride is oxidised according to either

$$2ZrN + 2O_2 = 2ZrO_2 + N_2 \quad (6)$$

or, in the absence of oxygen,

$$2ZrN + 4H_2O = 2ZrO_2 + N_2 + 4H_2 \quad (7)$$

with the same precedence as before.

If both Zr and ZrN are present, the oxidant consumption is split in the ratio 3:1 between ZrN and Zr.

The new species, Zr(O) (assumed to have the composition $ZrO_{0.4}$) and ZrN are calculated locally within the model and provided as output in separate files, since they are not presently accommodated in the code's register of quantities for output.

Before we turn our attention to the simulations, some remarks may be in order to make clear how much the nitriding model simplifies the real situation. The idealised picture in which the transport and reaction processes through the cladding are represented only by oxygen diffusion into an underlying zirconium to form a $ZrO_{0.4}$ sublayer which in turn reacts with nitrogen, ignores a number of additional processes and species. At temperatures and oxidant conditions similar to that occurred in QUENCH-16 and -18, a more complicated oxygen distribution in the cladding applies. Single rod experiments at KIT showed that α-Zr(O) can form both in the bulk of the ZrO_2 oxide and on its outer surface [30].

Other processes, not included in the model, further complicate the cladding composition and state. Like oxygen, nitrogen can also be taken up into the zirconium to produce a nitrogen-stabilised α-phase, somewhat analogous to oxygen stabilized α-Zr(O) [31] and which might be expected to affect the kinetics of the ongoing zirconium-gas reactions. Prior breakaway oxidation would lead to additional pathways through the porosity to promote access of gases to the unreacted zirconium. As observed by Park [17], this inhibits the formation α-Zr(O) and does not necessarily promote the nitriding. breakaway.

The porosity caused by breakaway and/or oxidation in the presence of nitrogen also promotes the take up of hydrogen released from oxidation in steam [32], which itself may affect the kinetics of both oxidation and nitriding in the presence of nitrogen. It should be noted that that this situation, typical for a reactor or spent fuel pool sequence, applied during QUENCH-16 and -18. However, the separate effects experiments which provided the data on which the current nitriding model was based [Park], were performed with oxygen used as a surrogate for steam.

4. Simulations of QUENCH-16 and -18* experiments

Code version and model options

The base code version used in all the simulations was MELCOR/1.8.6/3084/PSI, where 3084 refers to the release number and PSI denotes the PSI model for accelerated oxidation kinetics in the presence of nitrogen. Nitriding was later included in the PSI model, without further change to the code itself. The versions are referred to as pre-NT and NT. Both versions include the option of activating the model or not, via flags PSI=1 or PSI=0. With PSI=1, the accelerated oxidation kinetics can be activated or not, via flags nobrk=1 or nobrk=2.

Modelling of the QUENCH test section and boundary conditions

Instead of attempting to model the details the QUENCH-18 experimental set up and boundary conditions exactly, the same input was used as for -16 except for the -18 steam flow during the air ingress and the time to initiate reflood. This approach was considered viable for present purposes for the reasons discussed in section 2. In this way it is possible to examine most easily how well the model captures the influence of a steam-air mixture as opposed to air alone, without needing to take into account the effect of detailed differences between the experimental set ups. It is noted that the primary aim of the calculations is an assessment of the applicability of the model for simulating nitriding/re-oxidation in an air ingress sequence and capturing the main phenomenology, rather than to specifically compare the calculated results with empirical data. Despite the experimental differences, QUENCH-16 and -18 are sufficiently similar that comparison with the experimental results can be considered as credible for code assessment purposes.

To avoid confusion, the QUENCH-18 input used in the present simulations is from now on referred to as QUENCH-18*, an idealised representation of both the experimental test section and conditions.

Boundary conditions and modelling cases

The electrical power and flow rates are presented in Figure 6, showing both the gross electrical power and the power dissipated in the heater elements, i.e., excluding the external wiring and connections. The power was reduced shortly before the change in flow rates to enable the effect of air to be studied starting from a temperature below the rapid oxidation range.

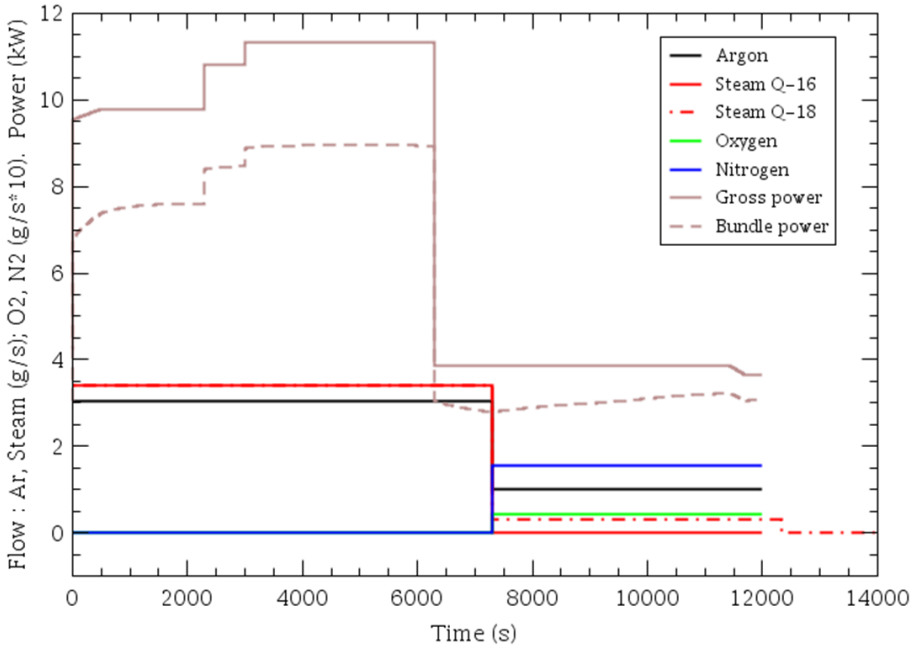

Figure 6: Boundary conditions for simulations

The simulated boundary conditions are slightly modified from the exact measured values in order to present a cleaner and more easily interpretable scenario for analysis. The gross electrical power is taken from the QUENCH-16 experiment [12], and is the same for both sets of simulations. The gas flow rates through the test section are similarly taken from the QUENCH-16 experiment. The unplanned additional flow of steam through the bundle, deduced from the measured hydrogen trace in QUENCH-16 and possibly occurring in QUENCH-18 as well, is not quantified and is not included in the simulations.

The only difference in boundary conditions between the simulations is the continued flow of 0.3 g/s steam (instead of zero) in QUENCH-18* during the air ingress phase which begins at 7310 s. The steam and argon flows were reduced at the time of start of the air ingress. The conditions at the start of air ingress are therefore identical.

Six simulations are presented for QUENCH-16, with both pre-NT and NT versions, while only the NT version for QUENCH-18*, with three input options as follows:

PSI=0 (PSI model not selected)

PSI=1,nobrk=2 (PSI model selected, no accelerated oxidation in nitrogen)

PSI=1, nobrk=1 (PSI model selected, accelerated oxidation in nitrogen)

With the pre-NT version, the case (PSI=1, nobrk=2) is physically equivalent to PSI=0, thus enabling direct comparison of the calculated air-ingress behaviours with and without activating the nitriding model. However, the PSI and non-PSI models use different the numerical solution methods, which may affect the calculation. With the NT version, nitriding is calculated with PSI=1 and so the nobrk=2 case is different from PSI=0. However, it provides the opportunity to test for compatibility between NT/PSI=1, NT/PSI=0 and pre-NT at times before nitriding has occurred. Comparison between physically equivalent cases is important as a test of non-regression with the PSI model, one of the reasons for the case nobrk=2. All the other inputs are the same.

Discussion of QUENCH-16 calculations and comparison with experiment

Figure 7 shows compares the measured cladding temperature at 750 mm on inner rod 11 with the six calculations. The first thing to notice is the remarkable level of agreement between all the simulations data during pre-oxidation and fairly close during the early part of the air ingress phase. The agreement is partly fortuitous, but essentially due to extensive use of the MELCOR code and input model in analyses of previous QUENCH experiments where conditions were similar. However, the NT version with PSI=1 gave slightly higher temperatures than pre-NT and NT/PSI=0.

The agreement is not as good during the early part of the air ingress phase when the flow conditions were somewhat novel, with the calculated temperature increasing more quickly than the data. There may have been an additional flow of steam through the bundle which would have affected the heat transfer. There was a broadly similar oxidation-induced acceleration, occurring at the same temperature as in the experiment but earlier in time. Again, the calculated temperatures are very close to each other until ca. 9500 s (ca. 10500 s in the experiment) when the nitriding cases rose more quickly after oxygen starvation and the onset of nitriding at this location. The NT cases reflect the experimental trends, but the earlier oxidation and nitriding meant that a higher temperature was calculated at the initiation of reflood.

The pre-NT cases all showed a rapid quench, but attempts to calculate the reflood using the NT version and nitriding activated all terminated with code failure. In order to examine how the transient might have continued, those cases were eventually without reflood.

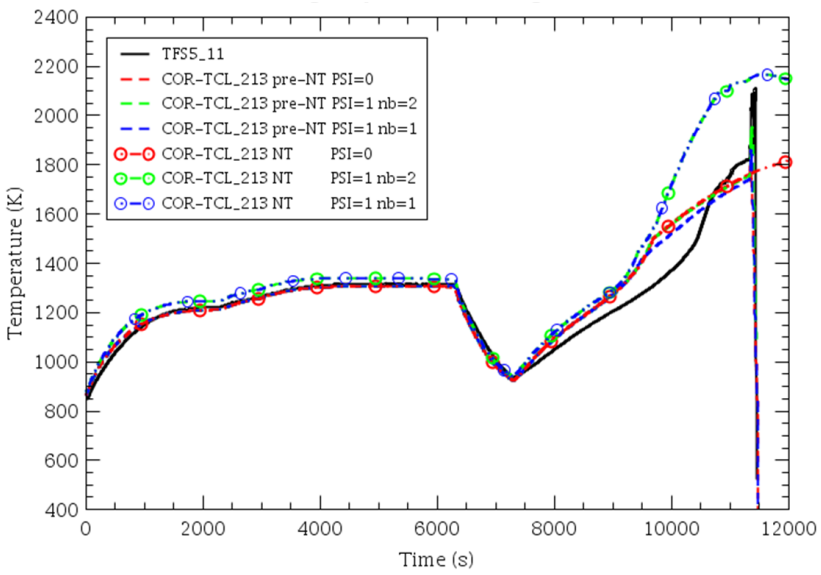

Figure 7: QUENCH-16 Experimental and calculated cladding temperature at 750 mm

A somewhat similar picture emerges at the 350 mm elevation, Figure 8, where the temperatures were lower during pre-oxidation and the early part of the air ingress phase. Again, the temperature during air ingress was overestimated in all the calculations. The acceleration in the heat-up occurred later than at 750 mm, in both the experiment and simulations though was more marked. Comparison between pre-NT and NT cases shows the calculated temperatures start to diverge at ca. 10000 s, suggest nitriding from about that time. This was not exhibited in the experiment, as oxygen starvation probably did not occur before reflood started. The pre-NT cases calculated a rapid quench at ca. 11500 s,

following reflood initiation, while the temperatures in NT cases continued to rise with and without the nitriding (PSI=1 and 0, respectively).

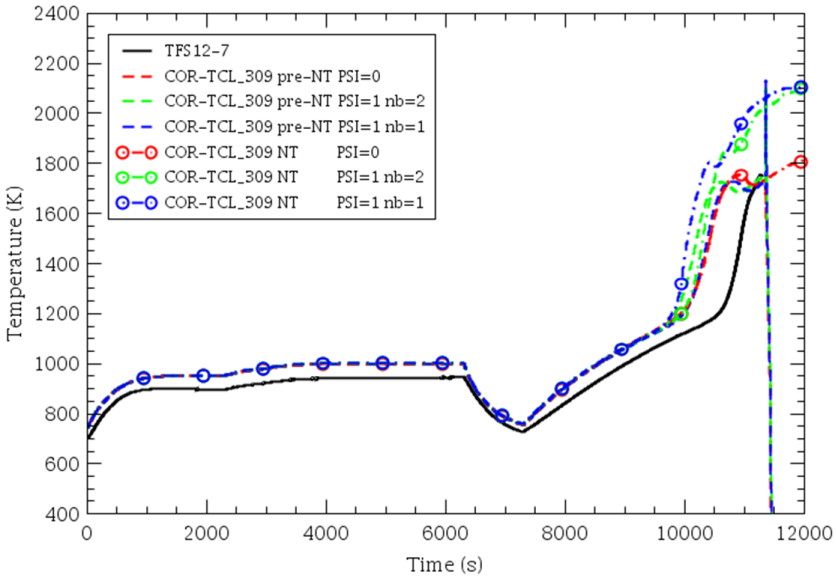

Figure 8: QUENCH-16 Experimental and calculated cladding temperature at 350 mm

Overall, the effect of oxidation and nitriding on the thermal response trends was well captured, but the higher calculated starting temperature prevents a clear quantitative comparison.

Figure 9 shows the hydrogen generation which was accurately calculated in all the non-NT cases during pre-oxidation but was systematically overestimated it by ca. 15% by the nitriding model. This discrepancy is a consequence of the way in which the oxidation kinetics were calculated by the nitriding model, in that the oxide thickness, instead of the mass gain, was used as the rate controlling parameter. Although this is the correct treatment, physically, the coefficients are not adjusted to take account of the thinner oxide layer when some of the oxygen is assigned to the alpha-Zr(O). Hence they no longer correspond to the empirically based mass gain correlation, in this case Cathcart-Pawel. This led to an over-counting of the oxygen uptake, hence hydrogen release. The extra heat release slightly affected the temperatures, as previously noted in Figure 6~~, and will be discussed in the next section~~. The

Obviously, no hydrogen should have been released during the air ingress, but the data reveal a small amount due to the additional steam flow (not include in the simulations). The data show a major oxidation occurred during reflood, which was not or only mildly reproduced in the simulations. Difficulties with calculating reflood excursion are encountered with all codes, including MELCOR, and are not a consequence of the nitriding model. Again, the NT cases were continued without initiation of reflood.

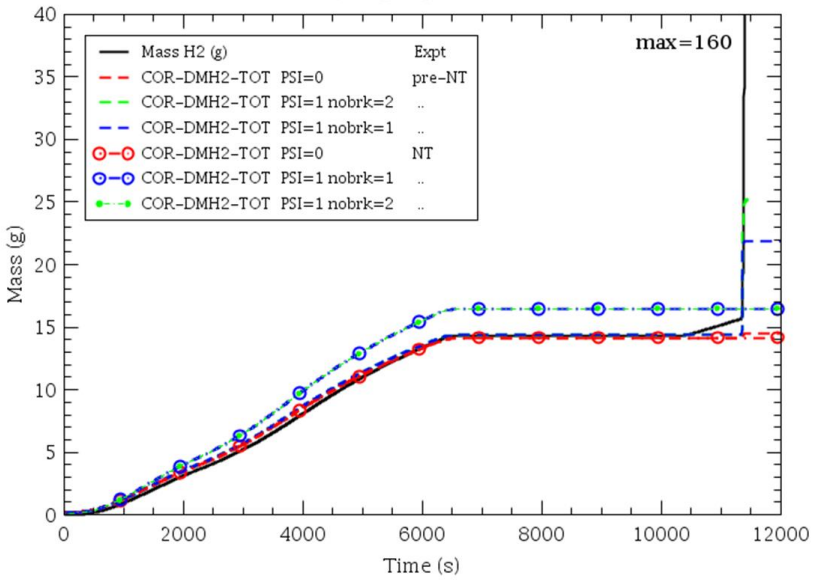

Figure 9: QUENCH-16 Experimental and calculated hydrogen generation

Figure 10 shows the calculated and observed offgas concentrations oxygen and nitrogen with the data. It is first noted the start of nitrogen consumption was almost coincidental with the onset of oxygen starvation, with calculation in agreement with experiment. The calculated timing also corresponds to the divergence in the temperature evolution between the pre-NT and NT calculations, when nitriding first became a source of heat. The oxygen time-profile during its consumption is well reproduced, except for the roughly 1000 s difference in timing.

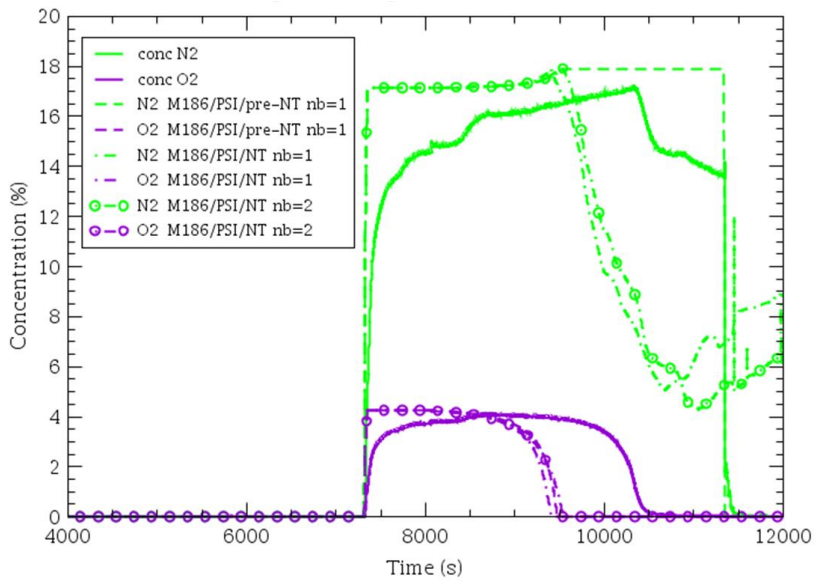

Figure 10: QUENCH-16 Experimental and calculated nitrogen and oxygen concentrations

The most noticeable difference is that the calculated nitrogen consumption is much higher than observed. Comparison of the initial decrease in nitrogen concentration suggests good agreement for the consumption rate, but it persisted much longer in the calculation. Part of the reason is that the calculated oxygen starvation occurred earlier that in the experiment and the starvation front progressed lower into the bundle, resulting in a larger nitriding region. Other factors, such as model uncertainty regarding the kinetics may be also be a factor.

Finally, the measured oxygen and nitrogen offgas concentrations increased very slowly to their nominal values at the start of the air ingress phase, suggesting some operational or facility related issues.

The modelled interplay between the reactions, over the entire test section, is revealed in Figure 11 which shows how the structural composition evolves during the sequence. However, it should be realised that the following description strictly applies only locally, and is less apparent when the effects at all the localities are aggregated. Starting with pure Zr, oxygen is uptaken to produce both ZrO_2 and $ZrO_{0.4}$ in a ratio of ca. 6:1, which remains almost constant into the air ingress phase until the onset of oxygen starvation and start of nitriding, resulting also in some of the $ZrO_{0.4}$ being converted to ZrO_2 and the remainder "recycling" the released oxygen to partially replenish the $ZrO_{0.4}$. At the same time oxygen diffuses from the ZrO_2 to produce more $ZrO_{0.4}$ at a slow rate. As the temperatures rise and the oxidation kinetics increase, the starvation front moves downward leading to an increase in the rate of nitriding. For a while the $ZrO_{0.4}$ fraction and the nitriding rate increases, until the nitriding has "consumed" most of the pre-existing $ZrO_{0.4}$ after which the continuing nitride formation is controlled by the rate at which $ZrO_{0.4}$ is formed by oxygen diffusion from the ZrO_2 into the Zr. Reference to Figure 9 shows the nitrogen uptake to increase and then decrease, while the $ZrO_{0.4}$ fraction stays roughly the same.

Finally, it is noted that the ZrO_2 corresponding to the hydrogen release, referred to as the "hydrogen equivalent mass" is almost exactly proportional to the calculated ZrO_2 only while the oxidation is by steam and under non-starved conditions. They are not equal because not all the oxygen is uptaken to produce ZrO_2. After that they are no longer proportional, and the calculated ZrO_2 overtakes the "hydrogen equivalent".

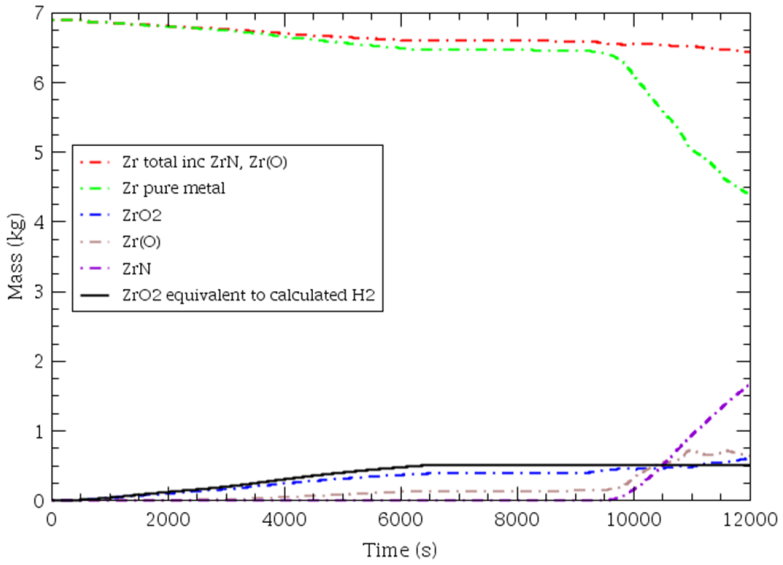

Figure 11: QUENCH-16 calculated cladding composition

Discussion of QUENCH-18* calculations and comparison with experiment

A limited set of calculations is presented, mainly concentrating on the influence effect of steam included with the air. Its aims were essentially to predict how a repeat QUENCH-16 would have evolved if it had been identically repeated except for the 0.3 g/s steam with the air, as an aid to interpretating the actual QUENCH-18, and to assess the model's applicability to air/steam mixtures. It is identical to QUENCH-16 up to the start of air ingress at ca. 7400 s.

Figure 12 compares the calculated and measured shroud temperatures at 750 mm, one of the few high temperature locations where the thermocouple survived through reflood. Agreement between all three calculations and data is very close during the pre-oxidation, similar to that for the heater rod in QUENCH-16 (Figure 4). There is likely to have been an element of "luck" involved, but it suggests that the numerous differences (test section configuration, boundary conditions) between the experiments tended to cancel out during the pre-oxidation, as was intended in the planning. It suggests that QUENCH-18* is an effective surrogate for -18, at least as regards the modelling aspects of present interest.

The case-case agreement continues for some time into the air ingress phase, but the simulations then start to accelerate as they gradually diverge from the data, similarly to QUENCH-16. The initial rate of reheating is slightly less than QUENCH-16, due to that higher coolant flow and the acceleration in temperature rise occurs slightly later, in both simulation and experiment. The two cases with nitriding (with and without accelerated oxidation in the presence of nitrogen) also diverge, with a runaway escalation leading to component melting in one case (nobrk=1), where the nitrogen-induced accelerated oxidation became a driver for the escalation, The other nitriding case (nobrk=2) failed soon after the start of nitriding. The case without nitriding continued and fairly well followed the data until ca. 11400 when the shroud was breached in the experiment and the measured temperature decreased. The temperature calculated without nitriding continued to rise, except for a short pause at ca. 10600 s, thought to be due to steam starvation at this elevation. None of the simulations calculated a large amount of nitriding, and hence showed only a minor effect on temperatures.

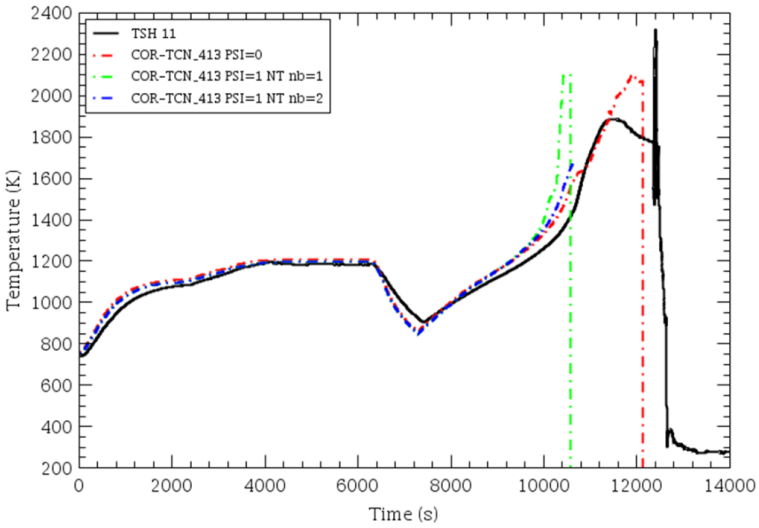

Figure 12: QUENCH-18(*) Experimental and calculated cladding temperature at 750 mm

Figure 13 compares the calculated hydrogen generation in the three NT cases with the data. All the cases overestimate the data during pre-oxidation, which was slightly lower than in QUENCH-16, the case without the nitriding model being closest and, as before, the NT model higher by about 15%. The curves again flatten during the cooling period and the early stage of air ingress before the onset of oxygen starvation after which steam begins to be consumed. From the beginning of hydrogen release at ca. 10500 s in the experiment, it is just a very short time before the steam is fully consumed. The no nitriding (PSI=0) case again gives the closest agreement, with the hydrogen release starting only slightly earlier and complete consumption slightly later than in the experiment. Both nitriding cases show hydrogen release and complete steam consumption noticeably earlier, followed by code failure. The non-NT case closely followed the experimental release right up until reflood, with a calculated 46 g compared with 57 g measured. A massive reflood excursion took place in the experiment, but was not captured by MELCOR.

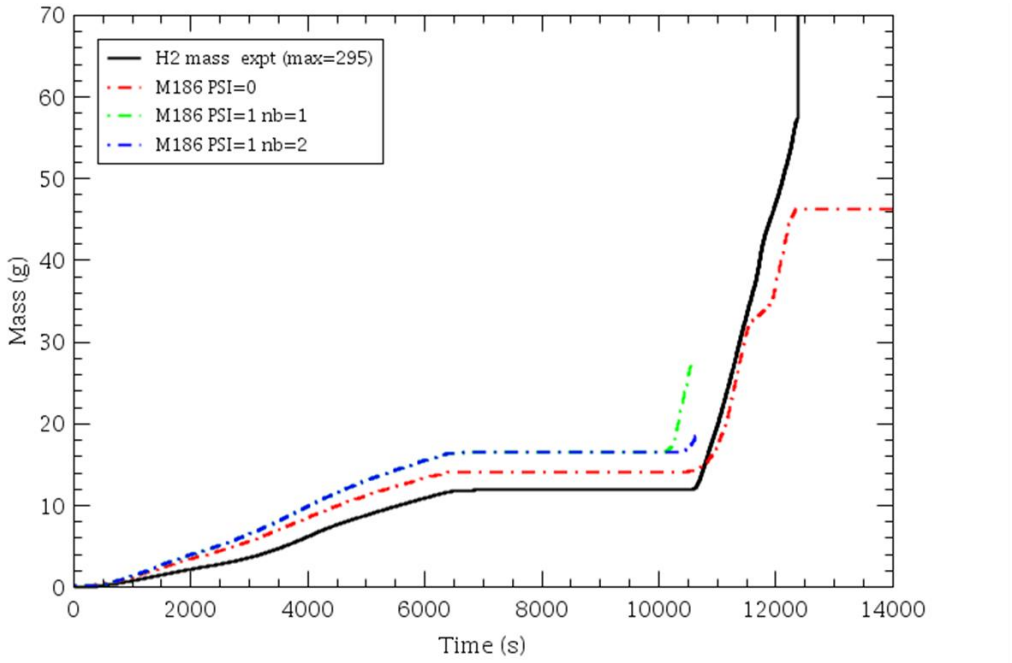

Figure 13: QUENCH-18(*) Experimental and calculated hydrogen generation

The offgas composition in terms of the molar fractions of hydrogen, oxygen, nitrogen, steam, and argon are shown in Figure 14 which includes hydrogen and steam in addition to just the oxygen and nitrogen displayed in Figure 9. Argon is shown for completeness, as well. As with QUENCH-16, the experimental values show some variations not occurring in the calculations. One probable cause is, again, condensation in parts of the system and subsequent re-evaporation when the humidity decreased at the start of the air ingress phase.

The calculated (case nobrk=2) oxygen consumption was again quicker than observed, though not by as much as it was in QUENCH-16 after taking into account the earlier switch from steam to air-steam mixture. A probable reason for the overestimated rate of oxygen consumption is that the concentration in the experiments was low, just a few percent, which is not taken into account by the model. Experiments at KIT [33] show a clear effect of concentration, for which an *ad hoc* correlation was derived [34] and included in a PSI local version of SCDAP/RELAP5 and used in an analysis of QUENCH-18 [35].

As expected, steam is not consumed until the effective onset of oxygen starvation, but once started, it is almost completely consumed within about 200 s, with the hydrogen concentration increasing almost exactly as the steam decreases. The calculated steam consumption and hydrogen release are in remarkably good agreement with the data, all things considered. In the experiment, the nitrogen concentration holds strictly its original value until all the oxygen is consumed but starts to decrease before complete steam consumption, and while the hydrogen release is still increasing. Therefore it appears that nitriding was occurring in the presence of steam. This calculated local oxidation in steam simultaneously with nitriding is not, in principle, accommodated in the model and would not be calculated. However, there is reason to believe this may happen, since hydrogen produced during steam oxidation decreases the oxygen partial pressure locally, and results in more favourable conditions for ZrN formation [36].

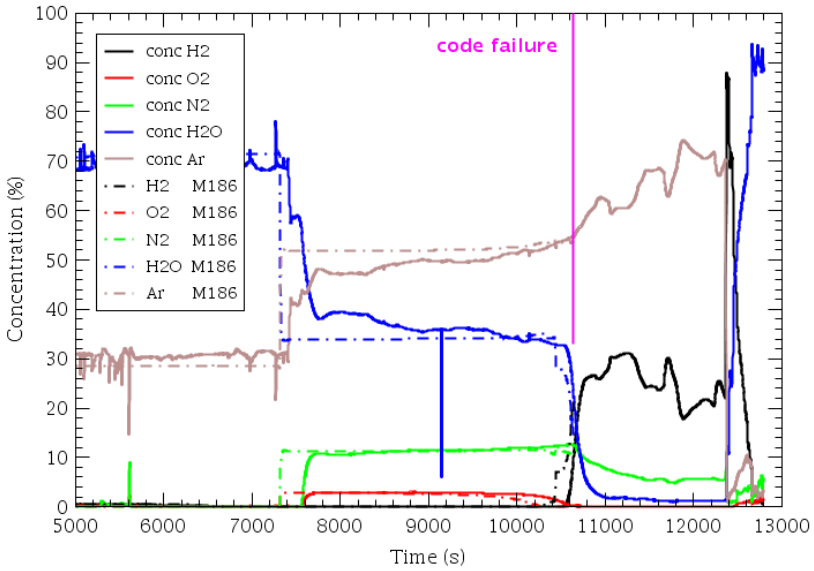

Figure 14: QUENCH-18(*) Experimental and calculated offgas composition

Both the experimental data and simulation show, somewhat surprisingly, the onset of nitrogen uptake at almost exactly the same time that the oxygen was fully consumed and while steam was still present. The experimental uptake increased to about to fifty percent, although it did not increase much in the simulation due to code failure soon after the onset of nitriding. This behaviour should not come as a surprise in the experiment, but is rather unexpected in the simulation, considering the reaction precedence. However, it may be connected with the way the oxidation and nitriding calculations are interfaced at low steam concentrations.

The code failure at an early stage during nitriding is of more concern, and the reason is not yet identified. Other attempts to simulate QUENCH-18* with the nitriding model also failed. A possible cause is that the QUENCH input model for MELCOR uses a single hydrodynamic control volume (CVH) to span more than one (COR) nodes, which are both sources and sinks for the reacting gases. This may lead to a conflict for the numerical solution algorithm when the oxygen starvation front passes across a CVH node which interfaces multiple COR nodes in different states of oxidation and/or nitriding.

5. Summary

The simulations demonstrate that the nitriding model works as intended in an air environment in conjunction with the PSI oxidation. model. Production of Zr(O) and ZrN are demonstrated. Unfortunately, attempts to simulate the reflood were not successful; consequently, it was not possible to demonstrate the reoxidation.

Consistency is demonstrated between simulations using the standard (i.e., not PSI version), the PSI pre-NT version, and NT version but with the nitriding model not activated.

There is a lack of consistency between the oxidation calculated using and not using the nitriding model, with about 15% more oxidation when the nitriding model. This is attributed to the reduced oxide thickness (the controlling factor with parabolic kinetics) as some of the oxygen is taken up in alpha-Zr(O).

There is no obvious and fully satisfactory solution. If the oxidation is not steam limited, then an available adjustment can be made to the kinetic coefficients to almost exactly recover the correlation based on oxygen mass gain. However, the correlations themselves for oxide and Zr(O) masses are not accurate under oxidant-limited conditions, and the adjustment may also be questionable.

The oxygen consumption rate is overestimated in comparison with the data for both experiments, leading to early starvation. This may be an effect of the low oxygen concentrations in the experiments which is not taken into account in the model. As a result, the calculated nitrogen uptake in QUENCH-16 and steam consumption in QUENCH-18 are premature, with impact on the ongoing escalations.

The nitrogen consumption is also overestimated in comparison with the data, which may be a consequence of the early calculated onset of nitriding.

The nitriding model calculation failed at an early stage during nitriding in QUENCH-18*, resulting in only a small amount of ZrN formed and no significant oxidation of ZrN. This problem was not encountered in the developmental assessment of the model, and may be a result of using a coarser hydraulic (CVH) noding than the core (COR) noding.

The oxidation excursions during reflood were not captured in any of the simulations. This limitation in not unusual in MELCOR simulation, especially with a coarse hydraulic noding as in the present model. However, even if the excursion were captured, it would not be possible to make a useful quantitative comparison with the reflood phases of the experiments, as the shroud was breached at this time in both experiments. This significantly affected the boundary conditions and was not represented in the model.

The code failed at start of reflood in all cases when the nitriding model was used to simulate QUENCH-16. This appears to to be due to numerical problems which, again, might be possibly avoided by a more detailed hydraulic noding.

Although QUENCH-18* does not correctly represent QUENCH-18 as regards the bundle configuration and boundary conditions, the similarity to the two experimental evolutions during pre-oxidation enables a meaningful comparison between simulated and experimental phenomenology and vindicates its use for model assessment.

6. Conclusions and recommendations

The newly developed and implemented model successfully captured most of the trends and phenomena for nitriding under transient conditions until reflood initiation, with the exception of cade failure during nitriding when steam is also present. The problem might not lie with the model itself.

Consideration of the reaction model specification alongside the QUENCH-18 data on offgas composition challenges the assumption that oxidation in steam takes precedence over nitriding when both gases are present.

The formation of alpha-Zr(O) is a key precursor to nitride formation, without which the nitriding would be very slow. This process is correctly calculated, at least qualitatively, by the model, as is the way it facilitates the nitriding. Quantitatively, there is a need for further experimental data on the nitriding process to address uncertainties in the kinetics and the reaction steps.

The alpha-Zr(O) formation, and consequently reduced oxide thickness, are normal processes during oxidation, and can result in the homogenisation (or near homogenisation) of moderately oxidised cladding under high temperature oxidant-starved conditions. Separately from nitriding or presence of nitrogen, this part of the model should make it possible to reproduce the observed reflood excursion following prolonged steam starvation, and predict the possibility of such an excursion in a reactor application.

Consistency with previous versions have been demonstrated for the present cases, except for this discrepancy regarding the oxidation. While the “alpha-modified” thickness is the correct quantity for the oxidation kinetics, the model needs to be modified as noted in the previous section.

Consideration of the reaction model specification alongside the QUENCH-18 data on offgas composition challenges the assumption that oxidation in steam takes precedence over nitriding when both gases are present. There is a case for an in-depth review of data on the reactions with steam and nitrogen, and perhaps further study, and to re-examine the reaction precedence.

For both nitriding and air oxidation models, there is a case for modifying the kinetics to take account of low oxygen/nitrogen concentrations, which applied in the QUENCH experiments and might be expected in a reactor accident or spent fuel accident.

The code failures means that the reoxidation part of the model cannot be assessed from these particular analyses, and the impact of water injection into an overheated core with oxidised/nitrided cladding cannot be assessed.

The numerical solution within nitriding model method should be examined in attempt to identify reasons for the failures during reflood and in steam+air environments. However, is not certain that the problems are in the model and numerical scheme themselves.

Although the present nitriding model has been implemented only in a PSI version of MELCOR, there is case for introducing the model into other system-level codes, for example SCDAP/RELAP5.

Some non-modelling improvements should be considered, notably inclusion of the new cladding composition quantities, Zr(O) and ZrN.

It is strongly recommended that the model is implemented in the general version of MELCOR, developed and maintained by Sandia National Labs. Indeed, their adoption of the model may be necessary to be able to properly address nitriding issues in reactor and spent fuel pool scenarios.

Despite the limitations identified above, the demonstrated success implies significant progress towards an effective model for reactor and spent fuel air ingress sequences.

References

[1] Powers, D., Kmetyk, L., Schmidt, R. (1994). A review of technical issues of air ingression during severe reactor accidents. Sandia National Lab., Report NUREG/CR-6218, SAND94-0731, Sandia National Lab., 1994.

[2] J. R. Wolf, J. L. Rempe, L. A. Stickler, G. E. Korth, D. R. Diercks, L. A. Neimark, D. W. Akers, B. K. Schuetz, T. L. Shearer, S. A. Chdvez, G. L. Thinnes, R. J. Witt, M. L. Corradini, J. A. Kos (1993). "TMI-2 Vessel Investigation Project Integration Report". NUREG/CR-6197, Idaho National Engineering Laboratory.

[3] K. Natesan, W.K. Soppet, S. Basu (2004). Low Temperature Air Oxidation Experiments at ANL, CSARP Meeting, Crystal City, VA, 3–4 May 2004.

[4] Hózer, Z., Szabó, E., Pintér, T., Varjú, I., Bujtás, T., Farkas, G., Vajda, N. (2009). Activity release from damaged fuel during the Paks-2 cleaning tank incident in the spent fuel storage pool. Journal of Nuclear Materials, 392, pp. 90-94. https://doi.org/10.1016/j.jnucmat.2009.03.049

[5] Duriez, C., Dupont, T., Schmet, B., Enoch, F. (2008). Zircaloy-4 and M5® high temperature oxidation and nitriding in air. Journal of Nuclear Materials, 380, pp. 30-45. https://doi.org/10.1016/j.jnucmat.2008.07.002

[6] Steinbrueck, M., Miassoedov, A., Schanz, G., Sepold, L., Stegmaier, U., & Stuckert, J. (2006). Experiments on air ingress during severe accidents in LWRs. Nuclear Engineering and Design, 236, pp. 1709-1719. https://doi.org/10.1016/j.nucengdes.2006.04.010

[7] Steinbrueck, M. (2009). Prototypical experiments relating to air oxidation of Zircaloy-4 at high temperatures. Journal of Nuclear Materials, 392, pp. 531-544. https://doi.org/10.1016/j.jnucmat.2009.04.018

[8] Steinbrueck, M., Grosse, M., Sepold, L., Stuckert, J. (2010). Synopsis and outcome of the QUENCH experimental program. Nucl. Eng. Design, 240, pp. 1714-1727. https://doi.org/10.1016/j.nucengdes.2010.03.021

[9] Fernandez-Moguel, L., Birchley, J. (2012). Simulation of air oxidation during a reactor accident sequence: Part 2 – Analysis of PARAMETER-SF4 air ingress experiment using RELAP5/SCDAPSIM. Ann. Nucl. Energy, 40, pp. 141-152. https://doi.org/10.1016/j.anucene.2011.10.018

[10] Hozer, Z., Windberg, P., Nagy, I., Maroti, L., Matus, L., Horvath, M., Pinter Csordas, A., Balasko, M., Czitrovszky, A., Jani, P. (2017). Interaction of Failed Fuel Rods Under Air Ingress Conditions. Nucl. Technol., 141, 244-256. https://doi.org/10.13182/NT03-A3365

[11] Zigh, A., Velazquez-Lozada, A. (2014). OECD-NEA Sandia Fuel Project (SFP). Retrieved from https://www.oecd-nea.org/jointproj/sfp.html

[12] Stuckert, J., Steinbrueck, M. (2014). Experimental results of the QUENCH-16 bundle test on air ingress. Progress in Nuclear Energy, 71, pp. 134-141. https://doi.org/10.1016/j.pnucene.2013.12.001

[13] Stuckert, J., Steinbrueck, M., Kalilainen, J., Lind, T., Birchley, J. (2021). Experimental and modelling results of the QUENCH-18 bundle experiment on air ingress, cladding melting and aerosol release. Nuclear Engineering and Design, 379. doi.org/10.1016/j.nucengdes.2021.111267

[14] Steinbrueck, M., Böttcher, M. (2011). Air oxidation of Zircaloy-4, M5® and ZIRLO™ cladding alloys at high temperatures. Journal of Nuclear Materials, 414, 276-285. https://doi.org/10.1016/j.jnucmat.2011.04.012

[15] Steinbrueck, M., Schaffer, S. (2015). High-Temperature Oxidation of Zircaloy-4 in Oxygen–Nitrogen Mixtures. Oxidation of Metals, 85, 245-262. https://doi.org/10.1007/s11085-015-9572-1

[16] Adorni, M., Herranz, L.E., Hollands, T., Ahn, K.-I., Bals, C., D'Auria, F., Horvath, G.L., Jaeckel, B.S., Kim, H.-C., Lee, J.-J., Ogino, M., Techy, Z., Velazquez-Lozad, A., Zigh, A., Rehacek, R. (2016). OECD/NEA Sandia Fuel Project phase I: Benchmark of the ignition testing. Nucl. Eng. Design, 307, 418-430. https://doi.org/10.1016/j.nucengdes.2016.07.016

[17] Park, S. Nitriding and Re-oxidation Behaviour of Zircaloy-4 at High Temperatures PhD Thesis, ETH Zürich, No. 27146, 2020. https://doi.org/10.3929/ethz-b-000459694

[18] Park, S., Lind, T., Birchley, J., Steinbrueck, M. (2022). Current understanding of high-temperature oxidation phenomena during air ingress scenarios. Proceedings of the 10th European Review Meeting on Severe Accident Research (ERMSAR2022). Karlsruhe, Germany.

[19] B.S. Jaeckel, B., Birchley, J., Lind, T., Steinbrueck, M., Park, S. (2023). Nitriding Model for Zirconium based Fuel Cladding in Severe Accident Codes. Journal of Nuclear Materials, 582, 154466. https://doi.org/10.1016/j.jnucmat.2023.154466

[20] Gauntt, R.O., et al., 2005. Code Manuals – Version 1.8.6, USNRC NUREG/CR 6119 Rev. 3, SAND2005-5713, Sandia National Laboratories, September.

[21] Birchley, J., Fernandez-Moguel, L. (2012). Simulation of air oxidation during a reactor accident sequence: Part 1 - Phenomenology and model development. Annals of Nuclear Energy, 40, 163-170. https://doi.org/10.1016/j.anucene.2011.10.019

[22] Fernandez-Moguel, L. (2015). Comparative assessment of PSI air oxidation model implementation in SCDAPSim3.5, MELCOR 1.8.6 and MELCOR 2.1. Annals of Nuclear Energy 81, 134–142. https://doi.org/10.1016/j.anucene.2015.03.015

[23] Fernandez-Moguel, L., Bals, C., Beuzet, E., Bratfisch, C., Coindreau. O., Hozer. Z., Stuckert, J., Vasiliev. A., Vryashkova, P. (2013). SARNET-2 WP5 Benchmark on Air Ingress Experiments QUENCH-10, -16.

[24] Malicki, M., Lind, T. (2023). Impact of PSI-KIT Nitriding model on hypothetical Spent Fuel Pool accident simulation, 55. https://doi.org/10.1016/j.net.2023.04.003

[25] Hollands, T. Bals, C., Beuzet, E., Le Belguet, Vasiliev, A., Kaliatka, T., Birchley, J., Steinbrueck, M., Stuckert, J., (2019). Pre- and Post-Test Simulations of the QUENCH-18 Bundle Experiment in the frame of the NUGENIA QUESA Project. The 9th European Review Meeting on Severe Accident Research (ERMSAR2019)

[26] Birchley, J., Jaeckel, B. (2022). First assessment of PSI nitriding model against QUENCH-Air Experiments. Proceedings of the 27th International QUENCH Workshop. https://doi.org/10.5445/IR/1000152245

[27] Pawel, R., Cathcart, J., McKee, R. (1979). The Kinetics of Oxidation of Zircaloy-4 in Steam at High Temperatures. Journal of the Electrochemical Society, 126, pp. 1105-1111.

[28] Schanz, G., Adroguer, B., Volchek, A. (2004). Advanced treatment of zircaloy cladding high-temperature oxidation in severe accident code calculations Part I. Experimental database and basic modelling. Nuclear Engineering and Design, 232, 7, pp. 5-84. https://doi.org/10.1016/j.nucengdes.2004.02.013

[29] Stuckert, J., Veshchunov, M. S. (2008). Behaviour of oxide layer of zirconium-based fuel rod cladding under steam starvation conditions. Scientific report FZKA-7373, Karlsruhe, 2008, https://www.doi.org/10.5445/IR/270071587)

[30] Steinbrueck, M. (2014). High-temperature reaction of oxygen-stabilized α-Zr(O) with nitrogen. Journal of Nuclear Materials, 447, pp. 46-55. https://doi.org/10.1016/j.jnucmat.2013.12.024

[31] Grosse, M.K., Steinbrueck, M., Pulvermacher, S., Schillinger, B. (2021). Enhanced Hydrogen Uptake and Reaction Kinetics during Oxidation of Zircaloy-4 in Nitrogen-Containing Steam Atmospheres. ASTM Special Technical Publication, STP 1622, pp. 621-642.

DOI: 10.1520/STP162220190009

[32] Grosse, M., Pulvermacher, S., Steinbrueck, M., Schillinger, B. (2018).In-situ neutron radiography investigations of the reaction of Zircaloy-4 in steam, nitrogen/steam and air/steam atmospheres. Physica B: Condensed Matter, 551, pp. 244-248.DOI: 10.1016/j.physb.2018.03.030

[33] Steinbrueck, M., U. Gerhards, M. Crosse, H. Leiste, S. Prestel, U. Stegmaier (2011). Recent separate-effects tests on oxidation of Zr alloys at KIT. 17th International QUENCH Workshop. ISBN:9783923704774 https://d-nb.info/1020156732

[34] Vryashkova, P., Groudev, P., Stefanova, A. (2013). Sensitivity study of Quench-16 experiment with MELCOR computer code. Proceedings of 19th Int. QUENCH Workshop, Karlsruhe, Nov. 2013, ISBN 978-3-923704-84-2

[35] Birchley, J, Stuckert, J., Steinbrueck, M., Grosse, M. (2019). Preliminary interpretative analysis of the QUENCH-18 bundle test using SCDAPSim/mod3.5. Annals of Nuclear Energy, 130, 20-33. https://doi.org/10.1016/j.anucene.2019.02.022

[36] Steinbrueck, M., Oliveira da Silva, F, M. Grosse (2017). Oxidation of Zircaloy-4 in steam-nitrogen mixtures at 600-1200°C. Journal of Nuclear Materials, 490, pp. 226-237. https://dx.doi.org/10.1016/j.jnucmat.2017.04.034

Acknowledgements

The authors wish to acknowledge the major efforts of Dr. Bernd Jaeckel*, in construction of the nitriding model and its implementation into the MELCOR code.
Thanks are due also to Dr. Leticia Fernandez-Mogul* and Mr. Larry Siefkin*** for their work on the PSI air oxidation model which provided the necessary framework within which to implement the nitriding model.

* formerly Paul Scherrer Institut, Switzerland
*** formerly Innovative Software Systems, USA

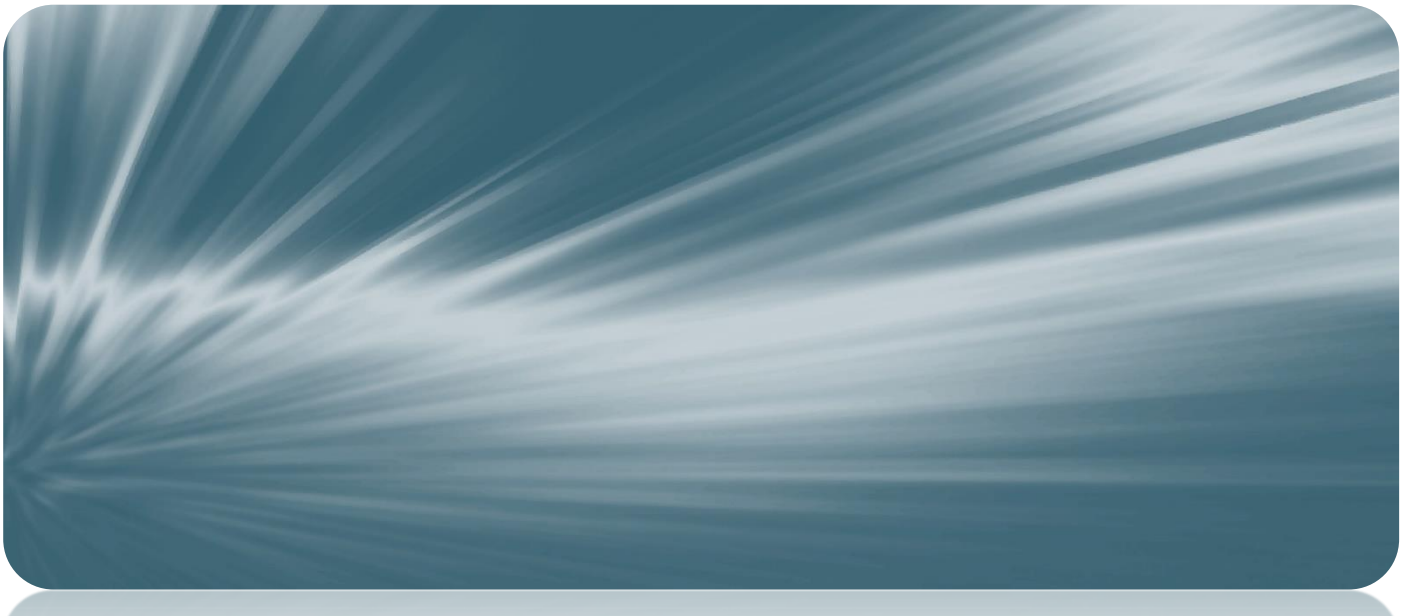

Abstract

The impacts of air ingress on nuclear safety have been a matter of concern for some forty years, and particularly so following such an incident at the Paks nuclear power station. As part of the effort to address these issues, an initial assessment of the recently developed PSI nitriding model was performed against the KIT air ingress experiments QUENCH-16 and -18. The study follows on from an experimental investigation on nitriding/reoxidation and the development of a model based on the results and its implementation into a version of MELCOR/1.8.6. The work was motivated by the extensive nitriding observed in previous integral experiments that were originally performed to address oxidation in air.

QUENCH-16 included a period of pre-oxidation in steam followed by an air (without steam) environment to address the continuing escalation up to and past the onset of oxidant starvation, after which nitriding is expected. QUENCH-18 was an approximate counterpart experiment in which the environment following pre-oxidation comprised a mixture of steam and air.

The capability to model the effect of a mixture of steam and air, addressed in QUENCH-18, is investigated qualitatively by repeating the QUENCH-16 simulation with the additional of steam flow corresponding to the QUENCH-18 conditions. An exact quantitative comparison between the QUENCH-16 and -18 results is not possible because of differences in bundle configuration.

Comparison between the QUENCH data and MELCOR simulations with and without the nitriding model show how the code captures the main trends and that the model captures the uptake of nitrogen and heat generation after all the oxygen is consumed, with formation of zirconium nitride (ZrN). No significant uptake of nitrogen was observed before oxygen starvation, in either the experiments or simulations. However, some nitrogen uptake was observed before steam starvation in QUENCH-18.

Some calculational difficulties emerged during the late stages of the simulations, including reflood, which are thought to be due to numerical issues. There is also an unintended difference in the calculated oxidation rate, due to an incorrect numerical treatment of the kinetics. Recommendations are proposed to address these shortcomings.